Int. J. Heat Mass Transfer. Vol. 9, pp. 1061–1074. Pergamon Press 1966. Printed in Great Britain

THE THERMAL CONDUCTIVITY OF SPHERICAL METAL POWDERS INCLUDING THE EFFECT OF AN OXIDE COATING

DAVID L. SWIFT*

Argonne National Laboratory, Argonne, Illinois

(*Received* 10 *June* 1965 *and in revised form* 21 *February* 1966)

Abstract—The effective thermal conductivity of a number of spherical metal powder–gas systems has been measured using a transient line source method. Variation of effective thermal conductivity with changes in gas pressure, temperature, and particle size was determined and the results compared with previous experiments. Uranium and zirconium powders were oxidized, and it was found that the effective thermal conductivity at atmospheric pressure decreased with extent of oxidation. An expression for randomly stacked spherical powders (void fraction = 0·40) was developed using the orthorhombic stacking arrangement and assuming linear heat flow. It was tested over a four-fold range in bulk solid conductivity to bulk gas conductivity ratio and found to give reasonable agreement. The treatment was extended to the case of metal particles with oxide coatings. It was found to agree with the uranium oxidation experiments in which a sharp decrease in effective thermal conductivity was noted in the initial stages of oxidation.

NOMENCLATURE

$a, b, c,$	constants for equation (7);
$d,$	particle diameter [cm];
$k,$	thermal conductivity [cal/cm s degC];
$L,$	mean free path [cm];
$q,$	heat input [cal/cm s];
$Q,$	heat flux [cal/cm^2 s];
$R_1,$	metal sphere radius;
$r, Z, \theta,$	cylindrical coordinates;
$T,$	temperature [°C];
$t,$	time [s];
$\alpha,$	thermal diffusivity [cm^2/s];
$\delta,$	source radius [cm];
$\Delta,$	constant for equation (7);
p, σ	constants for equation (7);
$\epsilon_v,$	void fraction;
$\epsilon_s,$	solid fraction.

RECENT studies of uranium powder ignition at Argonne National Laboratory [1] have been interpreted using the theory of thermal explosion proposed by Frank-Kamenetskii [2]. This theory defines a criterion for ignition in terms of the system geometry, the rate and heat of reaction, and the system thermal conductivity. It was therefore important to determine how the thermal conductivity of metal powders varies with temperature, pressure, particle size, and extent of oxidation. The thermal conductivities of several mesh fractions of uranium and zirconium powder have been measured as a function of pressure, temperature, and extent of oxidation and the results compared to a theoretical expression which was concurrently developed. In order to further test this expression, thermal conductivities of aluminum, copper, magnesium, nickel, and glass powders were also measured using nitrogen, hydrogen, helium, argon, methane, and Freon-12 as the interstitial gas.

EXPERIMENTAL METHOD

Powder thermal conductivity was measured using the transient line source method. This method was chosen because it is a rapid, absolute method which is suitable for measuring

* Present address: School of Hygiene and Public Health, The Johns Hopkins University, Baltimore, Maryland.

powder conductivity at various temperatures and pressures. The method makes use of the fact that the rate of heat transfer from a line source is a function of the thermal properties of the medium. It is unique among transient methods in that the experiment yields thermal conductivity directly, not thermal diffusivity. It was first used to measure the thermal conductivity of soil [3], and has since been used for insulating materials, [4], polymers [5], and various liquids [6, 7]. Van der Held and van Drunen [6] showed that the line temperatures at times t_1 and t_2 are related by the following expression:

$$T_2 - T_1 = (q/4\pi k)\ln\frac{t_2 - t_0}{t_1 - t_0} \qquad (1)$$

where T_1 = line temperature at t_1, °C;
T_2 = line temperature at t_2, °C;
q = heat input, cal/cm s;
k = thermal conductivity, cal/cm s degC;
t = time, s;
t_0 = zero time correction.

The zero time correction is necessary because of the finite radius of the source. It was shown [6] to have an approximate value of $\delta^2/4\alpha$ where δ is the source radius and α is the powder thermal diffusivity. It can be found by trial as that time correction which makes T vs. ln $(t - t_0)$ linear. The powders were contained in a stainless steel cylindrical cell, 2 in long and 0·75 in diameter (see Fig. 1). A 0·025-in OD hypodermic tube was soldered along the axis of the cylinder; this tube contained a 36-gauge constantan heating wire and two 40-gauge iron–constantan thermocouples. Two reference thermocouples were attached to the cell exterior. The heating wire was powered by a d.c. supply capable of supplying up to 0·5 amps at 40 volts. The resistance of the heating wire was measured independently using a bridge, while the current during an experiment was determined from the voltage drop across a 3-ohm precision resistor in series with the heating wire.

The cell was enclosed in a furnace which is capable of maintaining a temperature of 300°C. Provision was made to measure thermal conductivity using several gases at absolute pressures ranging from 10^{-5} to 5×10^3 mm (approximately 100 psig). The output of the two iron–constantan couples, connected as a thermopile, was recorded on a Brown potentiometer recorder. A typical thermal conductivity determination took one minute and gave a maximum

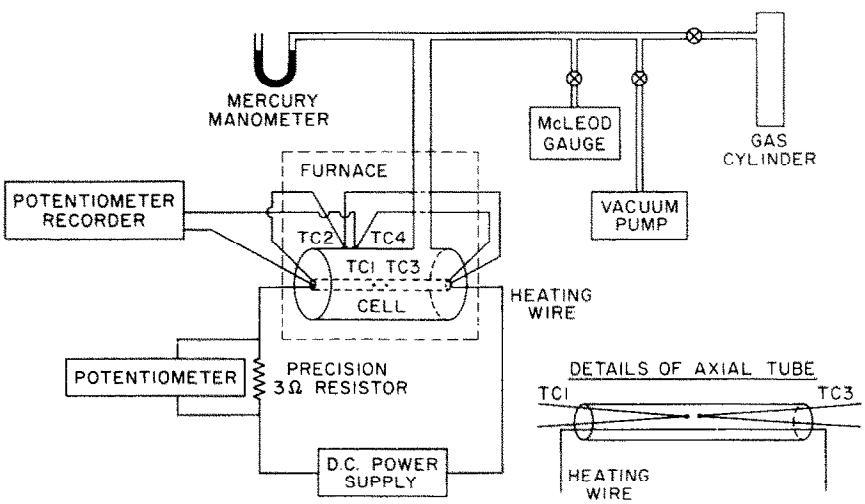

FIG. 1. Powder thermal conductivity apparatus.

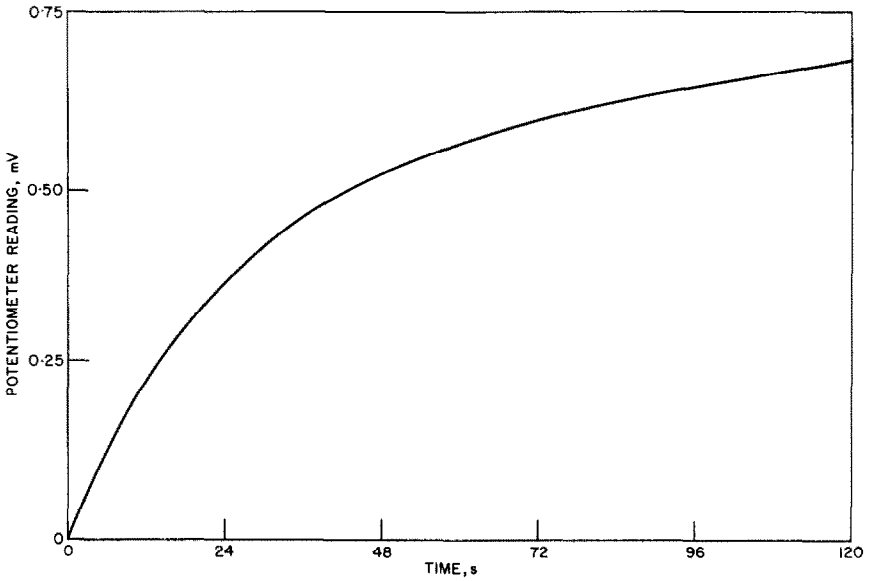

FIG. 2. Typical potentiometer trace.

center line temperature rise of approximately 15 degC. A temperature–time trace for one of the zirconium experiments is shown in Fig. 2. After about one minute of measurement, the time–temperature relationship is no longer represented by equation (1) because of the boundary effect of the cell.

Each time the cell was filled with powder, it was gently tapped until no further reduction in bulk volume was noted. In all cases, this was found to give a void fraction of 0·40. Furthermore, reproducible values of thermal conductivity were obtained in repeated tests of this packing procedure using the same powder.

MATERIALS AND PREPARATION

The spherical uranium powder used in these experiments was obtained from the National Lead Company and was separated into mesh fractions using standard screen techniques. The sphericity of the powder was verified microscopically. A chemical analysis of the uranium is listed elsewhere [1]. The powders were normally kept in a helium drybox to prevent gradual oxidation. In order to oxidize a powder, it was spread over the bottom of a Petri dish and placed in an oven at 150°C. The extent of oxidation was determined by weighing.

Reactor grade zirconium in the form of $\frac{1}{16}$ in wire was submitted to the Linde Company for preparation of the zirconium powder. This powder was likewise seived into a number of fractions of spherical powder. Because zirconium oxidizes much slower than uranium, it was necessary to oxidize the zirconium in porcelain dishes in a furnace at either 300 or 600°C depending on the particle size. Other powder materials used included aluminum, copper, magnesium, nickel, and Pyrex. The sources and size fractions of these materials are listed in Table 1.

The gases used in the experiments were nitrogen, helium, hydrogen, argon, methane, and Freon-12, all of commercial purity or better.

RESULTS AND DISCUSSION

A. Unoxidized uranium powder

Initial experiments with uranium powders were conducted using three mesh fractions ($-16 +20$, $-70 +80$, and $-230 +325$). Ther-

mal conductivities in nitrogen gas were measured at atmospheric pressure and at temperatures ranging from 25°C to 300°C. The results, shown in Fig. 3, indicate a linear increase of thermal conductivity with temperature, and an increase of conductivity with increasing particle size. Thermal conductivity of five uranium mesh fractions at 25°C in N_2 were measured at pressures from 5×10^{-5} to 5×10^{3} mm and the results are shown in Fig. 4. These curves are similar in shape to those obtained by Masumuni and Smith [8] for glass powders and stainless steel shot in that at high and low pressures the thermal conductivity does not change with pressure.

Table 1. Powder materials

Materials	Form	Mesh size	Supplier
Aluminum	Grained ingot	−30 +45	Alcoa Aluminum Company
Copper	Nearly spherical	−30 +35	Belmont Smelting and Refining Co.
Magnesium	Spherical	−100 +200	Valley Metallurgical Processing Co.
Nickel	Spherical	−230 +325	Linde Company
Pyrex	Beads	−140 +200	Minnesota Mining and Manf. Co.

According to the kinetic theory of gases [9] the thermal conductivity of a gas is essentially independent of pressure. However, at low pressures, the gas mean free path, L, is appreciable with respect to the particle diameter, d, resulting in free molecular conduction so that the overall powder conductivity decreases. The pressure above which conductivity is constant can be characterized by a critical Knudsen number, L/d. The critical Knudsen number for the uranium powders in nitrogen, was approximately 3×10^{-4}, while Deissler and Eian [10] report a critical Knudsen number of 7×10^{-4} for magnesium oxide powder in air, helium, and argon. The limiting high pressure conductivity, $\bar{k}$, is seen from Fig. 4 to increase as the particle size increases. The conductivity at very low absolute pressures, hereafter denoted k_0, is apparently the contact conductivity of the particles. It likewise increases with particle size, but is never more than approximately 5 per cent of the value of $\bar{k}$. At high pressures, essentially all of the heat conduction is by a series path through both gas and solid.

In a recent paper, Butt [11] has presented a theoretical expression for two-phase thermal

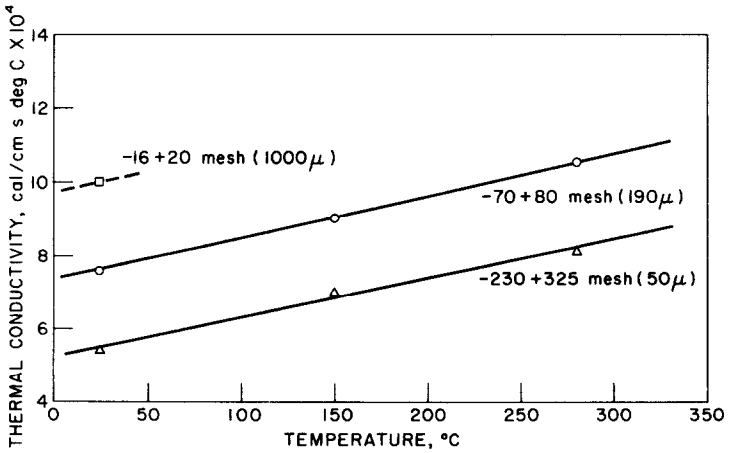

FIG. 3. Thermal conductivity of unoxidized uranium powder in nitrogen at atmospheric pressure.

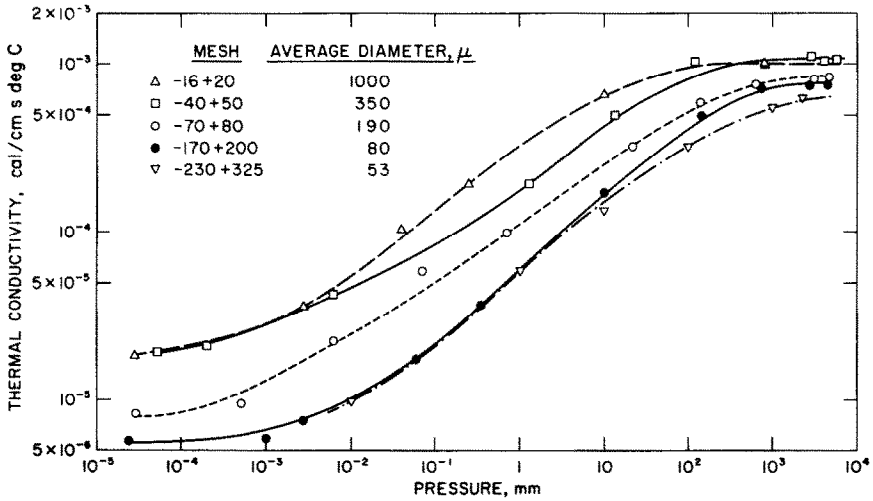

FIG. 4. Thermal conductivity of unoxidized uranium powder at 25°C in nitrogen.

conductivity, including the effect of gas pressure. For the system under consideration, using the symbols defined above, Butt's equation for the effective thermal conductivity is:

$$k = \frac{\bar{k}}{(1 + 2L/d)} + k_0. \qquad (2)$$

At high pressure, $2L/d \ll 1$ and $k \sim \bar{k}$ since $\bar{k} \gg k_0$. At moderately low pressures, $2L/d \gg 1$ and $k \sim kd/2L$, while at very low pressure, $kd/2L \ll k_0$ so that $k \sim k_0$. These three regions are clearly seen in Fig. 4. Butt's theory predicts that in the region of moderately low pressure $d \log k/d \log L = -1$; however the maximum experimental slope in Fig. 4 is $d \log k/d \log L = -0{\cdot}42$, approximately a square root dependence upon pressure. The data of Masamuni and Smith [8] for stainless steel shot likewise show a maximum slope of $-0{\cdot}43$ while for glass spheres the maximum slope is $-0{\cdot}25$.

The thermal conductivity of the $-70 +80$ mesh uranium powder was measured at 24°C in several gases at pressures ranging from 10^{-2} to 5×10^{-3} mm. The results are shown in Fig. 5. The $\bar{k}$ values for these gas–powder systems were in the same order as the gas thermal conductivities, i.e. $k_{He} > k_{CH_4} > k_{N_2} > k_{Ar}$. At low pressure the thermal conductivities are nearly equal; this is consistent with the assumption that k_0 is a contact conductivity and that the gas at this pressure contributes very little to the overall conductivity.

B. Oxidized uranium powders

Thermal conductivity measurements were performed with two mesh fractions of oxidized uranium powder as a function of the extent of oxidation. The results of these experiments are shown in Figs. 6 and 7, plotted as a function of nitrogen pressure at 25°C. The limiting high pressure conductivity $\bar{k}$, falls off rapidly at low oxidation extent, and then more gradually as the oxidation reaches completion at an O/U atom ratio of 2·44. It is interesting to note that the value of k_0 remains essentially unchanged throughout the oxidation. Since uranium oxides are poorer thermal conductors than uranium metal this indicates that the particle contact is somewhat better with the oxide-coated particles. Figure 8 shows how the conductivity of the medium and fine mesh powders at 25°C and atmospheric pressure changes with extent of oxidation.

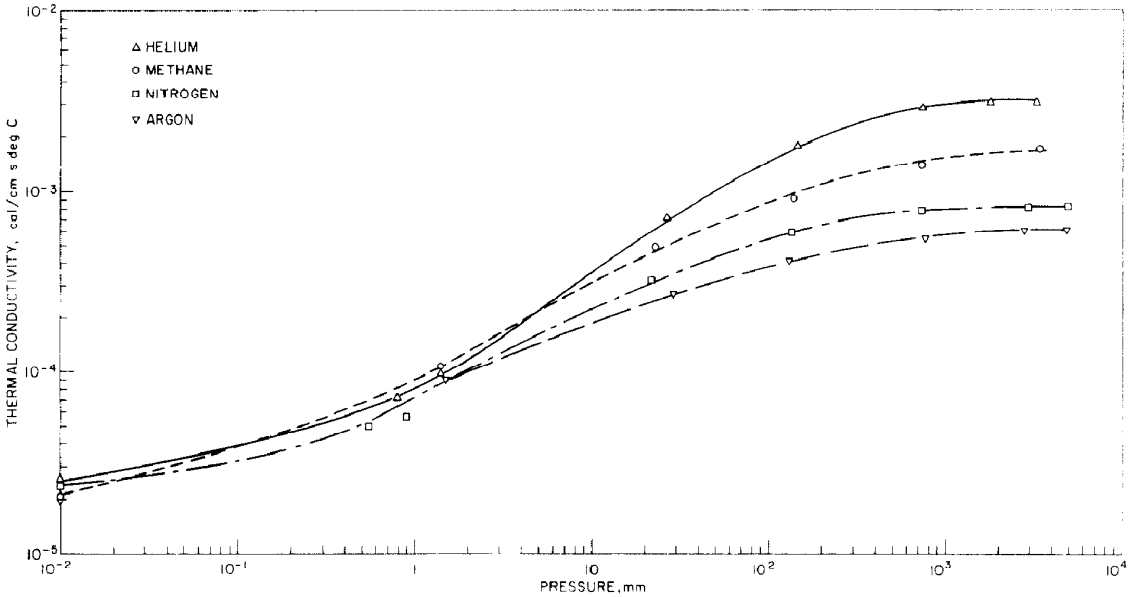

FIG. 5. Thermal conductivity of uranium powder (−70 + 80 mesh) at 25°C in various gases.

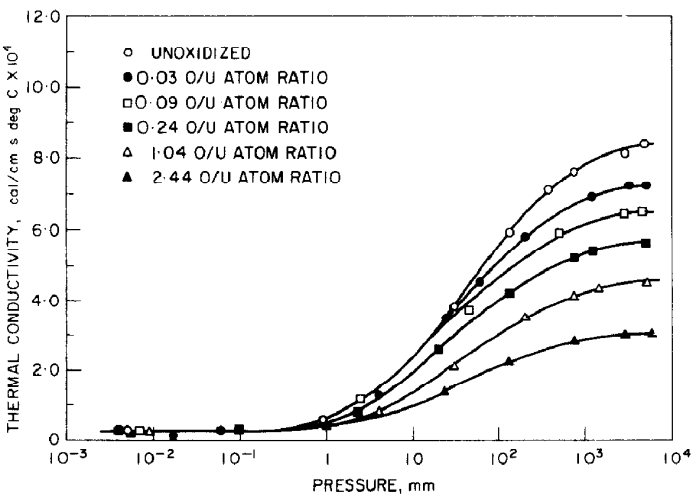

FIG. 6. Thermal conductivity of oxidized uranium powder (−70 + 80 mesh) in nitrogen at 25°C.

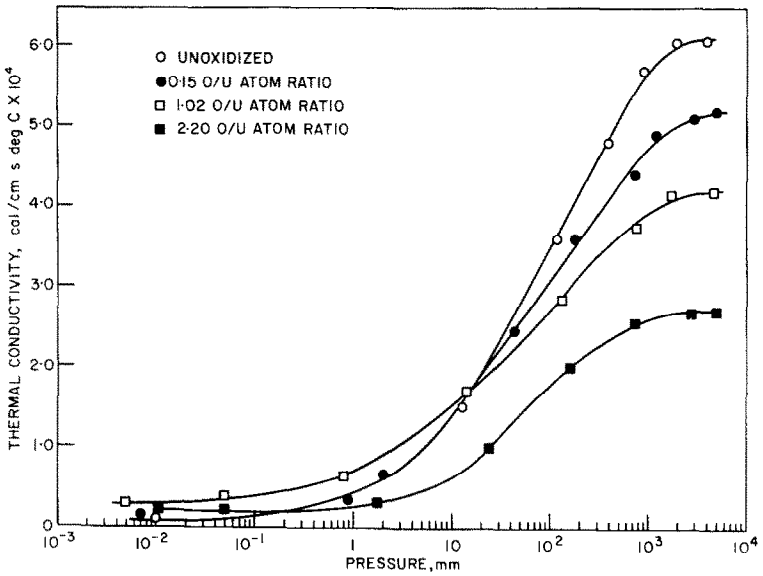

FIG. 7. Thermal conductivity of oxidized uranium powder (−230 + 325 mesh)

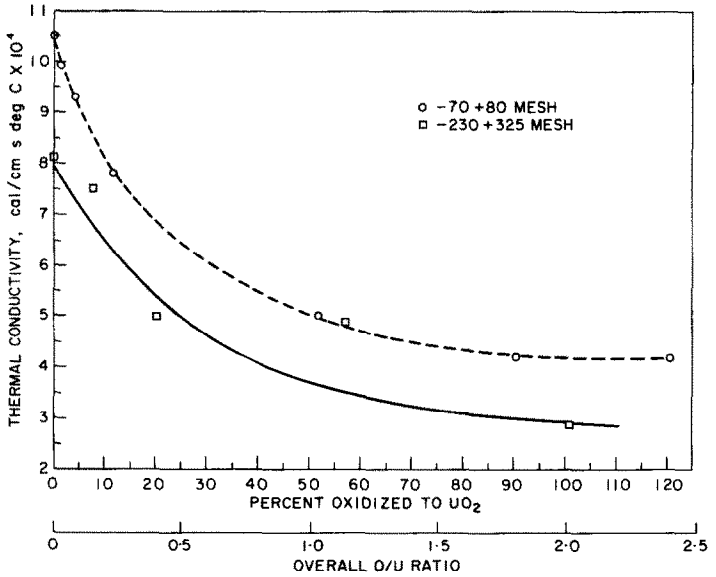

FIG. 8. Thermal conductivity of oxidized uranium powder in nitrogen at 25°C and 1 atm.

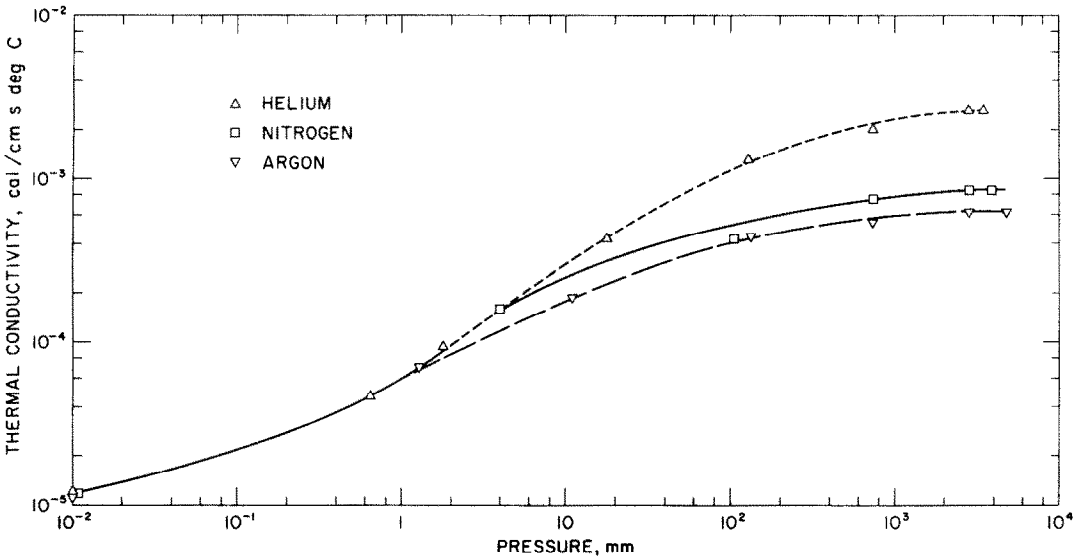

FIG. 9. Thermal conductivity of zirconium powder in various gases at 25°C (−70 + 80 mesh).

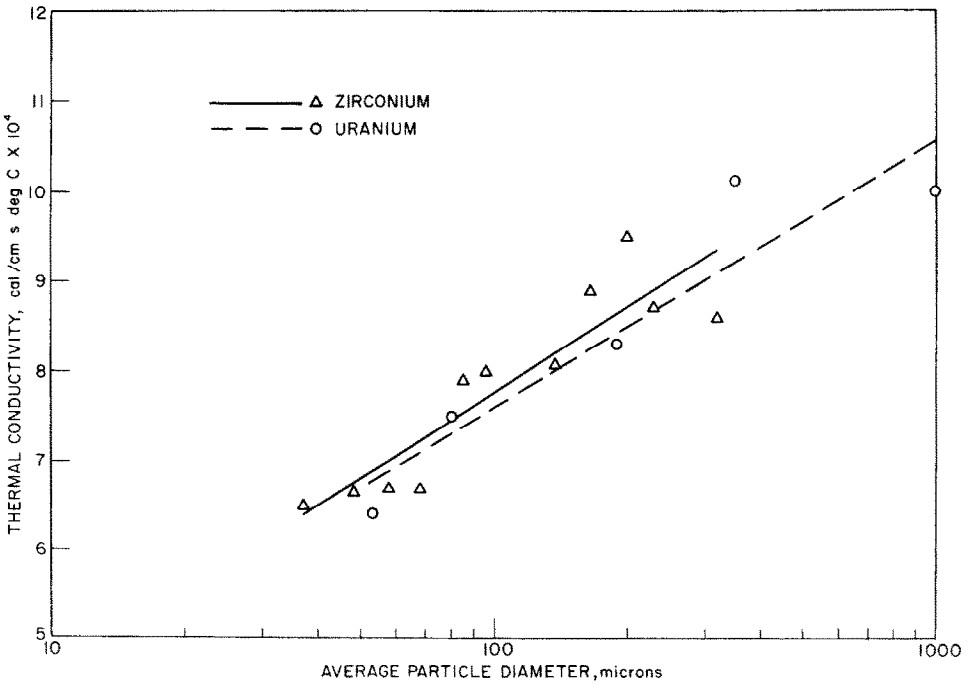

FIG. 10. Limiting high pressure thermal conductivity of uranium and zirconium powder at 25°C in nitrogen.

C. Zirconium powders

The thermal conductivity of −70 +80 mesh zirconium powder was measured at various pressures of helium, nitrogen, and argon at 25°C; the results in Fig. 9 show that as with uranium, the $\bar{k}$ values increase with increasing gas conductivity and the k_0 values are identical. Values of $\bar{k}$ were measured for several zirconium size fractions in nitrogen at 25°C and are plotted along with uranium powder data in Fig. 10 as a function of average particle size. Both uranium and zirconium powders show the tendency for $\bar{k}$ to increase with increasing particle size. Measurements of oxidized −70 +80 mesh zirconium powder were performed at 25°C in nitrogen. As shown in Fig. 11, they exhibit a decrease of $\bar{k}$ with extent of oxidation similar to that found with oxidized uranium powder; however, the effect is not as marked at first as with uranium (see Figs. 6 and 7). This is probably due to the fact that zirconium oxide is a more compact and adherent coating than the uranium oxide.

D. Other powder materials

In order to test a correlating equation (see below), the thermal conductivity of aluminum, copper, magnesium, nickel, and Pyrex glass powders were measured at pressures high enough (generally 100 psig) such that $\bar{k}$ values were obtained. The experiments were performed at 25°C using hydrogen, helium, methane, nitrogen, argon, and Freon-12. The results of these experiments are presented in Table 2.

THEORETICAL CORRELATION

There have been numerous theoretical equations for powder thermal conductivity suggested. Several treatments (e.g. Rayleigh [12], Russell [13], Woodside [14], and Deissler and Eian [10]) begin with an assumed stacking arrangement, and the effective conductivity is obtained as a function of the bulk conductivities of the two phases, and the void fraction. This type of treatment is only applicable for predicting $\bar{k}$. The equations developed by Masumuni and

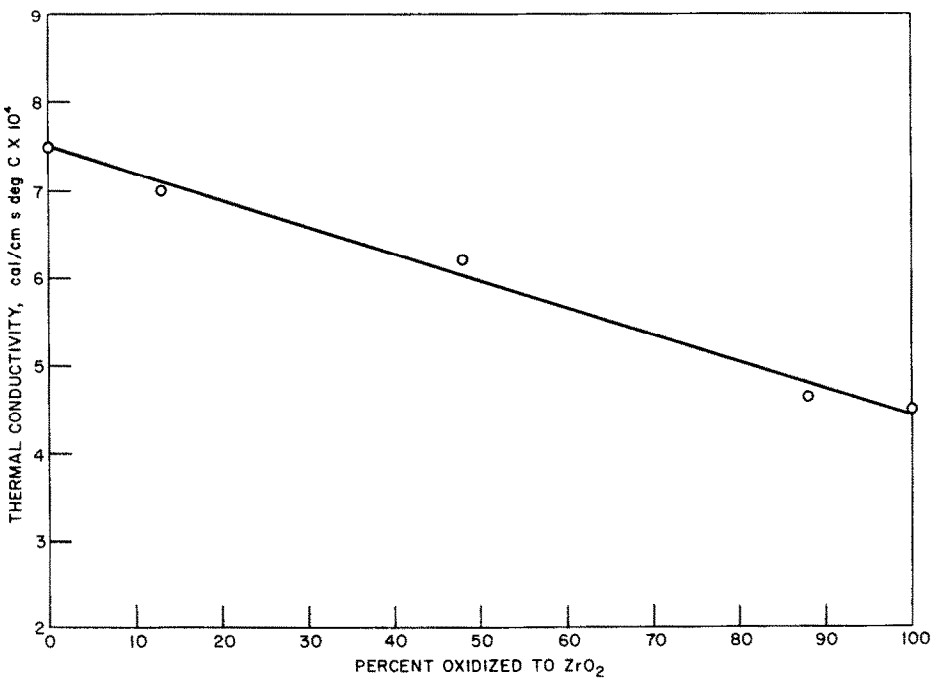

FIG. 11. Thermal conductivity of oxidized zirconium powder (−70 + 80 mesh) at 25°C and 1 atm.

Table 2. Thermal conductivity data for test of orthorhombic model

Solid	Gas	Solid conductivity k_s	Gas conductivity k_g	Power conductivity $\bar{k}$	k_s/k_g	$\bar{k}/k_g$
Aluminum	Argon	0·561*	$4{\cdot}18 \times 10^{-5}$	$6{\cdot}10 \times 10^{-4}$	$1{\cdot}34 \times 10^{4}$	14·6
	Nitrogen		$6{\cdot}10 \times 10^{-5}$	$8{\cdot}70 \times 10^{-4}$	$9{\cdot}20 \times 10^{3}$	14·3
Copper	Freon-12	0·982*	$2{\cdot}35 \times 10^{-5}$	$4{\cdot}60 \times 10^{-4}$	$4{\cdot}18 \times 10^{4}$	19·6
	Argon		$4{\cdot}18 \times 10^{-5}$	$7{\cdot}85 \times 10^{-4}$	$2{\cdot}35 \times 10^{4}$	18·8
	Nitrogen		$6{\cdot}10 \times 10^{-5}$	$1{\cdot}05 \times 10^{-3}$	$1{\cdot}61 \times 10^{4}$	17·2
	Methane		$7{\cdot}95 \times 10^{-5}$	$1{\cdot}50 \times 10^{-3}$	$1{\cdot}24 \times 10^{4}$	18·9
	Helium		$3{\cdot}55 \times 10^{-4}$	$3{\cdot}95 \times 10^{-3}$	$2{\cdot}77 \times 10^{3}$	11·1
	Hydrogen		$4{\cdot}25 \times 10^{-4}$	$4{\cdot}80 \times 10^{-3}$	$2{\cdot}31 \times 10^{3}$	11·3
Magnesium	Freon-12	0·406*	$2{\cdot}35 \times 10^{-5}$	$2{\cdot}40 \times 10^{-4}$	$1{\cdot}73 \times 10^{4}$	10·2
	Argon		$4{\cdot}18 \times 10^{-5}$	$5{\cdot}00 \times 10^{-4}$	$9{\cdot}71 \times 10^{3}$	12·0
	Nitrogen		$6{\cdot}10 \times 10^{-5}$	$6{\cdot}50 \times 10^{-4}$	$6{\cdot}65 \times 10^{3}$	10·7
	Methane		$7{\cdot}95 \times 10^{-5}$	$9{\cdot}70 \times 10^{-4}$	$5{\cdot}11 \times 10^{3}$	12·2
	Helium		$3{\cdot}55 \times 10^{-4}$	$3{\cdot}40 \times 10^{-4}$	$1{\cdot}14 \times 10^{3}$	9·58
	Hydrogen		$4{\cdot}25 \times 10^{-4}$	$3{\cdot}70 \times 10^{-3}$	$9{\cdot}55 \times 10^{2}$	8·70
Nickel	Freon-12	0·241*	$2{\cdot}35 \times 10^{-5}$	$4{\cdot}70 \times 10^{-4}$	$1{\cdot}03 \times 10^{4}$	20·0
	Argon		$4{\cdot}18 \times 10^{-5}$	$6{\cdot}70 \times 10^{-4}$	$5{\cdot}76 \times 10^{3}$	16·0
	Nitrogen		$6{\cdot}10 \times 10^{-5}$	$8{\cdot}35 \times 10^{-4}$	$3{\cdot}95 \times 10^{3}$	13·6
	Methane		$7{\cdot}95 \times 10^{-5}$	$9{\cdot}90 \times 10^{-4}$	$3{\cdot}03 \times 10^{3}$	12·5
	Helium		$3{\cdot}55 \times 10^{-4}$	$2{\cdot}95 \times 10^{-3}$	$6{\cdot}79 \times 10^{2}$	8·31
	Hydrogen		$4{\cdot}25 \times 10^{-4}$	$3{\cdot}55 \times 10^{-3}$	$5{\cdot}67 \times 10^{2}$	8·35
Uranium	Argon	0·0590*	$4{\cdot}18 \times 10^{-5}$	$6{\cdot}10 \times 10^{-4}$	$1{\cdot}41 \times 10^{3}$	14·6
	Nitrogen		$6{\cdot}10 \times 10^{-5}$	$8{\cdot}20 \times 10^{-4}$	$9{\cdot}67 \times 10^{2}$	13·4
	Helium		$3{\cdot}55 \times 10^{-4}$	$3{\cdot}20 \times 10^{-3}$	$1{\cdot}66 \times 10^{2}$	9·01
Zirconium	Argon	0·0621*	$4{\cdot}18 \times 10^{-5}$	$6{\cdot}20 \times 10^{-4}$	$1{\cdot}48 \times 10^{3}$	14·8
	Nitrogen		$6{\cdot}10 \times 10^{-5}$	$8{\cdot}40 \times 10^{-4}$	$1{\cdot}02 \times 10^{3}$	13·8
	Helium		$3{\cdot}55 \times 10^{-4}$	$2{\cdot}60 \times 10^{-3}$	$1{\cdot}75 \times 10^{2}$	7·32
Pyrex		$2{\cdot}50 \times 10^{3}$†	$2{\cdot}35 \times 10^{-5}$	$2{\cdot}80 \times 10^{-4}$	106	11·9
	Argon		$4{\cdot}18 \times 10^{-5}$	$4{\cdot}00 \times 10^{-4}$	59·8	9·57
	Nitrogen		$6{\cdot}10 \times 10^{-5}$	$5{\cdot}00 \times 10^{-4}$	41·0	8·20
	Methane		$7{\cdot}95 \times 10^{-5}$	$7{\cdot}00 \times 10^{-4}$	31·4	8·81
	Helium		$3{\cdot}55 \times 10^{-4}$	$1{\cdot}05 \times 10^{-3}$	7·04	2·96
	Hydrogen		$4{\cdot}25 \times 10^{-4}$	$1{\cdot}35 \times 10^{-3}$	5·88	3·18
	Water (l)		$1{\cdot}44 \times 10^{-3}$	$1{\cdot}50 \times 10^{-3}$	1·74	1·04

* Obtained from *Thermophysical Properties Research Center Data Book*, Volume 1, Purdue University, 1963.
† Obtained from *Handbook of Chemistry*, 10th Edition, N. A. LANGE, Ed., McGraw-Hill, New York. 1961.

Smith [8] are applicable to the transition region between k_0 and $\bar{k}$, but depend upon a knowledge of the thermal accommodation coefficient, the contact conductivity, k_0, and the fraction of a cross sectional area taken up by the solids.

The randomly stacked spherical powders used in the present experiments had measured void fractions of 0·40. Among regular packing structures, the orthorhombic structure, void fraction 0·395, best approximates this condition. Furthermore, McGeary [15] observed that uniform size spheres tend to stack in the orthorhombic arrangement. We therefore consider a unit cell of the orthorhombic structure shown in Fig. 12 with a unit area normal to

heat flow, a unit temperature difference, and a calculated thickness of 0·76 units. Following the treatment of Deissler and Eian [10], we assume no bending of heat flux lines. First considering the areas where heat flows through

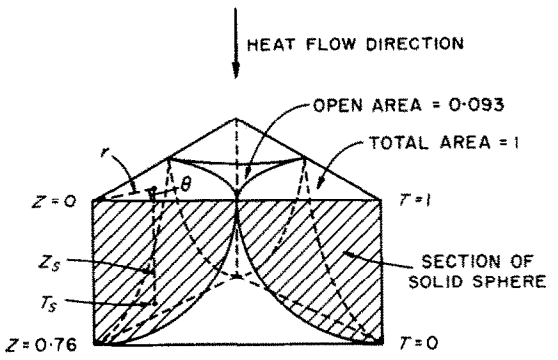

FIG. 12. Orthorhombic unit cell for thermal conductivity calculation.

both solid and gas, we can write the heat flow rate, dQ, through an area $r\,dr\,d\theta$ in terms of the sphere surface temperature, T_s, and the solid and gas path length, Z_s and $(0{\cdot}76 - Z_s)$:

$$dQ = k_s r\,dr\,d\theta \frac{(1 - T_s)}{Z_s} = k_g r\,dr\,d\theta \frac{T_s}{(0{\cdot}76 - Z_s)} \tag{3}$$

where k_s = solid conductivity,
k_g = gas conductivity.

Eliminating T_s and integrating over the three circular segments, [using the substitution $Z_s = \sqrt{(0{\cdot}577 - r^2)}$] we obtain the heat flow through the solid and gas in series. Adding to this the heat flow through the area whose projected volume contains only gas, and multiplying this total heat flow by 0·76, we obtain an expression for the effective conductivity:

$$\bar{k}/k_g = 0{\cdot}577\pi \{(\lambda_s - 1)^{-1} - (\lambda_s - 1)^{-2} \ln \lambda_s\} + 0{\cdot}093 \tag{4}$$

where $\lambda_s = k_g/k_s$.

This relationship is shown in Fig. 13 and compared with the correlation obtained by Deissler and Eian [10] for a void fraction of 0·40. The data for unoxidized uranium and zirconium powder and for the other powder materials listed in Table 2 is plotted on Fig. 13. An experimental point in the lower left-hand corner of Fig. 13 corresponds to the system Pyrex–water. The data show some scatter but appear to fit equation (4) reasonably well.

This correlation relationship and the experimental data can be compared also to the theory proposed by Butt, referred to above. For the limiting high pressure conductivity, Butt's equation for these systems is

$$\bar{k} = \epsilon_v^2 [1 + 4\epsilon_v \epsilon_s] k_g + \epsilon_s^2 k_s \tag{5}$$

where ϵ_v = void fraction
ϵ_s = solid fraction.

Inserting the appropriate values, we obtain:

$$\frac{\bar{k}}{k_g} = 0{\cdot}314 + \frac{0{\cdot}36}{\lambda_s}. \tag{6}$$

This reduces to a linear relationship between $\bar{k}/k_g$ and k_s/k_g at large values of k_s/k_g. At high values of k_s/k_g, equation (4) displays a much weaker dependence of $\bar{k}/k_g$ upon k_s/k_g, represented by the slope $d \log \bar{k}/k_g / d \log k_s/k_g = 0{\cdot}145$. At $k_s/k_g = 10^3$, equation (6) predicts $\bar{k}/k_g = 360$, more than an order of magnitude larger than the data and two correlation lines shown in Fig. 13. The experimental data of Deissler and Eian (not shown in Fig. 13) are in reasonably good agreement with their correlation; thus, it appears that the theoretical expression of Butt is not in good agreement with the data of this investigation and of Deissler and Eian, particularly at high values of k_s/k_g. It should be noted that the critical test of a two phase conductivity expression is at large k_s/k_g, where the conductivities of the two phases are vastly different.

OXIDE-COATED PARTICLES

This treatment has been extended to the case where the particle has a coating of different

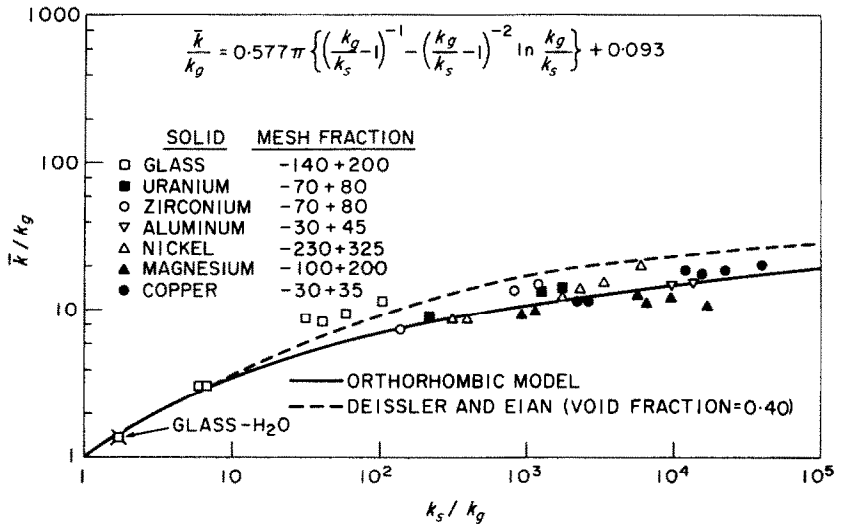

FIG. 13. Test of equation for powder thermal conductivity, $\bar{k}$, orthorhombic model.

thermal conductivity, k_c. In this case, the effective thermal conductivity is a function of the three conductivities, k_g, k_s, and k_c, and the fraction of the particle volume which is coating. The expression for $\bar{k}/k_g$ is obtained in the same manner as equation (3); it consists of three terms: (1) conduction through gas, (2) conduction through gas and coating, (3) conduction through gas, coating, and solids as follows:

$$\frac{\bar{k}}{k_g} = 0.093 + 0.76\pi\left\{\frac{p}{(\lambda_c - 1)} - \frac{0.76}{(\lambda_s - 1)^2}\ln\left[\frac{(\lambda_s - 1)p + 0.76}{0.76}\right] + 0.597\, I_t\right\} \tag{7}$$

where

$$I_t = \frac{(\sigma - p)}{c} - \left(\frac{p^4 b}{2a^2} + \frac{b}{2c^2}\right)\ln\left[\frac{a + b\sigma + c\sigma^2}{a + bp + cp^2}\right] + \frac{p^4 b}{a^2}\ln\frac{\sigma}{p} + \frac{p^3}{a}\left(\frac{p - \sigma}{\sigma}\right) + \left[\left(\frac{b^2 - 2ac}{2c^2}\right) + p^4\left(\frac{b^2 - 2ac}{2a^2}\right)\right]\frac{1}{\sqrt{-\Delta}} \times \ln\left(\frac{2c\sigma + b - \sqrt{-\Delta}}{2c\sigma + b + \sqrt{-\Delta}}\right)\left(\frac{2cp + b + \sqrt{-\Delta}}{2cp + b - \sqrt{-\Delta}}\right)$$

and $\sigma = 0.76 + R_1$;
$p = \sqrt{0.577 - R_1^2}$;
$a = p^2/2\,(1 - 2\lambda_c + \lambda_s)$;
$b = 0.76$;
$c = \frac{1}{2}(\lambda_s - 1)$;
$\Delta = 4ac - b^2$;
$\lambda_c = k_g/k_c$.

R_1 is the radius of the inner metal sphere and can be simply related to the coating volume fraction.

Equation (7) was applied to the oxidized uranium (−70 +80 mesh) powder–nitrogen system using the values $k_g = 6.1 \times 10^{-4}$ cal/cm s degC for nitrogen, $k_s = 7.4 \times 10^{-2}$ cal/cm s degC for uranium, and $k_0 = 1.46 \times 10^{-3}$ cal/cm s degC for the oxide coating. This last value for the oxide coating was obtained from equation (4) using the experimentally measured conductivity of the fully oxidized powder (O/U atom ratio 2.44). The results of these calculations are shown in Fig. 14. The predicted behavior of the thermal conductivities corresponds well with the experimentally obtained conductivities, showing an initially sharp de-

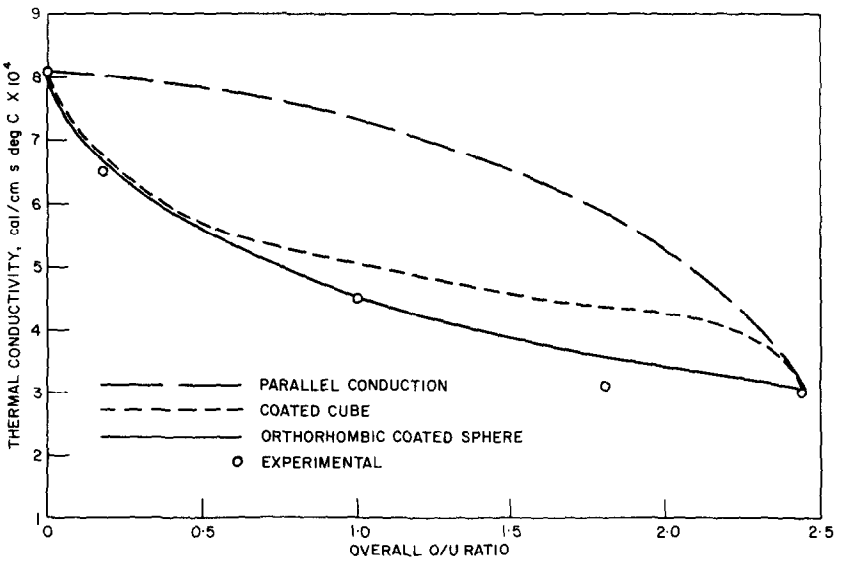

FIG. 14. Effect of oxide coating on thermal conductivity of uranium powder (−70 + 80 mesh) in nitrogen at 25°C ($\bar{k}$).

crease followed by a more gradual decrease with increasing extent of oxidation. Predicted thermal conductivities using two other models are also shown in Fig. 14, neither of which give as good agreement with the experimental points as the orthorhombic model. The first of these is a simple parallel conduction model, while the second is a combination parallel–series conduction model assuming the particle is a coated cube.

ACKNOWLEDGEMENTS

The author acknowledges the work of Mr. Paul Krause in measuring the powder thermal conductivities and oxidizing the powders. He also acknowledges the interest and advice of Dr. Louis Baker Jr. who initially suggested this study.

REFERENCES

1. M. TETENBAUM, L. MISHLER and G. SCHNIZLEIN, Uranium powder ignition studies, *Nucl. Sci. Engng* **14**, 230–238 (1962).
2. D. A. FRANK-KAMENETSKII, *Diffusion and Heat Exchange in Chemical Kinetics*, p. 236. Princeton University Press, Princeton (1955).
3. B. STALHANE and S. PYK, Ny metod for Bestamning av Varmelednings-koefficienter, *Tek. Tidskr.* **61**, 389–393 (1931).
4. B. H. VOS, Measurement of thermal conductivity by a non-steady-state method, *Appl. Scient. Res.* **A5**, 425–438 (1954).
5. W. M. UNDERWOOD and R. B. MCTAGGERT, The thermal conductivity of several plastics measured by an unsteady state method, *Chem. Engng Prog. Symp. Ser.-Heat Transfer* **56**, 261–268 (1959).
6. E. F. M. VAN DER HELD and F. G. VAN DRUNEN, A method of measuring the thermal conductivity of liquids, *Physica, 's Grav.* **15**, 865–881 (1949).
7. J. K. HORROCKS and R. MCLAUGHLIN, Non-steady-state measurements of the thermal conductivities of liquid polyphenyls, *Proc. R. Soc.* **A273**, 259–274 (1963).
8. S. MASAMUNI and J. M. SMITH, Thermal conductivity of beds of spherical particles, *Ind. Engng Chem. Fund.* **2**, 136–143 (1963).
9. SIR J. JEANS, *Kinetic Theory of Gases*, p. 47. C.U.P., London (1959).
10. R. G. DEISSLER and C. S. EIAN, Investigation of effective thermal conductivity of powders, NACA RM E52C05 (1952).
11. J. BUTT, Thermal conductivity of porous catalysts, *A.I.Ch.E. Jl* **11**, 106–112 (1965).
12. LORD RAYLEIGH, On the influence of obstacles arranged in rectangular order upon the properties of a medium, *Phil. Mag.*, **34**, 481–502 (1892).
13. H. W. RUSSELL, Principles of heat flow in porous insulators, *J. Am. Ceram. Soc.* **18**, 1–5 (1935).
14. W. WOODSIDE, Calculation of the thermal conductivity of porous media, *Can. J. Phys.* **36**, 815–823 (1958).
15. R. K. MCGEARY, Mechanical packing of spherical particles, *J. Am. Ceram. Soc.* **44**, 513–521 (1961).

Résumé—La conductivité thermique effective de quelques systèmes gaz-poudre de sphères métalliques a été mesurée en utilisant une méthode transitoire avec source linéique. La variation de la conductivité thermique effective a été déterminée lorsque la pression du gaz, la température et la taille de la particule changent, et les résultats ont été comparés avec des expériences antérieures. Des poudres d'uranium et de zirconium ont été oxydées et l'on a trouvé que la conductivité thermique effective à la pression atmosphérique diminuait lorsque l'oxydation était plus profonde. Une expression pour des poudres de sphères empilées au hasard (porosité = 0,40) a été exposée en employant un empilement orthorhombique et en supposant un flux de chaleur linéaire. On l'a vérifiée dans une gamme de rapport de la conductivité globale du solide à la conductivité globale du gaz allant du simple au quadruple et l'on a trouvé que l'accord était raisonnable. Le traitement a été étendu au cas de particules métalliques revêtues d'oxydes. On a trouvé un accord avec les expériences d'oxydation d'uranium dans-lesquelles une diminution brutale dans la conductivité thermique effective a été rema quée dans les étapes initiales de l'oxydation.

Zusammenfassung—Die scheinbare Wärmeleitfähigkeit einer Reihe kungelförmiger Metallpulver-Gassysteme wurde gemessen mit einer instationären Methode und linienförmiger Wärmequelle. Änderungen der scheinbaren Wärmeleitfähigkeit mit Änderung des Druckes, der Temperatur und der Partikelgrösse wurden bestimmt und die Ergebnisse mit früheren Versuchen verglichen. Uran und Zirkonium wurden oxydiert, wobei sich zeigte, dass die scheinbare Wärmeleitfähigkeit bei Atmosphärendruck mit dem Oxydationsgrad abnahm. Ein Ausdruck für wahllos angeordnete kugelförmige Pulver (Hohlraumanteil 0,40) wurde entwickelt, wobei eine orthorombische Stapelordnung benützt und ein linearer Wärmefluss angenommen wurde. Dieser Ausdruck wurde bis zum vierfachen Wert des Verhältnisses der Festkörperleitfähigkeit zur Gaswärmeleitfähigkeit geprüft, wobei sich annehmbare Übereinstimmung ergab. Die Untersuchung wurde auf Metallpartikel mit Oxydschichten ausgedehnt. Es zeigte sich Übereinstimmung mit den Versuchen der Uranoxydation, in denen ein starker Abfall der scheinbaren Wärmeleitfähigkeit in den Anfangsstadien der Oxydation auftrat.

Аннотация—С помощью метода нестационарного линейного источника измерена эффективная теплопроводность ряда систем сферические металлические порошки–газ. Установлена зависимость эффективной теплопроводности от изменений давления газа, температуры и размеров частиц. Результаты сравнивались с данными предыдущих экспериментов. Окислялись порошки урана и циркония, и было найдено, что с увеличением степени окисления при атмосферном давлении эффективная теплопроводность снижалась. На основе результатов для ромбической укладки и в допущении линейности теплового потока получено выражение для беспорядочной укладки сферических порошков (коэффициент пористости = 0,40).

Проверка выражения показала хорошее совпадение данных. Метод развит на случай металлических частиц с окисными покрытиями. Получено хорошее согласие с экспериментами по окислению урана, где наблюдалось резкое снижение эффективной теплопроводности в начальных стадиях окисления.